

Time-Resolved Fluorescence of Human Aortic Wall: Use for Improved Identification of Atherosclerotic Lesions

Jean-Michel I. Maarek, DR ENG,^{1*} Laura Marcu, PhD,^{1,2} Michael C. Fishbein, MD,³ and Warren S. Grundfest, MD²

¹Department of Biomedical Engineering, University of Southern California, Los Angeles, California 90089

²Laser Research & Technology Development Laboratory, Cedars Sinai Medical Center, Los Angeles, California 90048

³Departments of Pathology and Laboratory Medicine, UCLA School of Medicine, Los Angeles, California 90095

Background and Objective: This study characterized aortic time-resolved fluorescence spectra for stratified levels of atherosclerosis and proposed interpretation of spectrotemporal variations in terms of histologic changes.

Study Design/Materials and Methods: Fluorescence emission transients were measured at 370–510 nm (337 nm excitation) on 94 excised human aortic samples, ranging from normal to advanced fibrous atherosclerotic lesion. Global analysis yielded a three-exponential approximation of the time-resolved spectra from which average lifetime and decay-associated spectra were derived.

Results: Average lifetime at 390 nm gradually increased from 2.4 ± 0.1 nsec (normal aorta) to 3.9 ± 0.1 nsec (advanced lesion). Fluorescence intensity was markedly decreased above 430 nm in intermediate and advanced lesions. Spectral intensity associated with the intermediate decay increased at 470–490 nm for early and intermediate lipid-rich lesions.

Conclusion: Time-resolved fluorescence spectra of aortic samples presented distinctive features for each atherosclerotic lesion type, which could serve as characteristic markers for optical analysis of the aortic wall. *Lasers Surg. Med.* 27:241–254, 2000. © 2000 Wiley-Liss, Inc.

Key words: fluorescence spectroscopy; atherosclerosis; nitrogen laser; global analysis; time-dependent fluorescence decay; lifetime; decay-associated spectra; optical biopsy

INTRODUCTION

Laser-induced fluorescence spectroscopy has been widely researched as a nondestructive optical approach for medical diagnostic. In particular, application to the identification of atherosclerotic lesions has been explored in vitro and in situ by using continuous-wave [1–4] and time-resolved techniques [5–8]. Most studies examined advanced fibrous atherosclerotic lesions and described characteristic differences in the continuous-wave spectra of such lesions when compared with normal arterial wall [1,2]. A few studies investigated the emission of less advanced lipid-rich

lesions to conclude that distinct features could also be found in their fluorescence spectra [9–11].

Contract grant sponsor: American Heart Association, Greater Los Angeles Affiliate; Contract grant number: 1082-GI; Contract grant sponsor: Charles Lee Powell Foundation; Contract grant sponsor: Biomedical Simulation Resource at the University of Southern California; Contract grant sponsor: Medallions Group, Cedars Sinai Medical Center.

*Correspondence to: Jean-Michel I. Maarek, Department of Biomedical Engineering, University of Southern California, Los Angeles, CA 90089-1451.
E-mail: jmaarek@bmsrs.usc.edu

Accepted 6 April 2000

Spectral characteristics of healthy and diseased arterial tissue were interpreted in terms of arterial wall content in specific fluorescent compounds. The structural protein elastin abundant in the intima and the media of normal arteries was the most important contributor to the fluorescence of healthy arterial wall [2,10]. Collagen in the fibrous cap of advanced lesions determined the emission characteristics of severely atherosclerotic tissue [2,3]. Fluorescent lipids and lipoproteins imparted recognizable features to the spectra of lipid-rich lesions [11]. To our knowledge, no study to date has fully investigated the fluorescence spectra for the whole sequence of lesions that separates normal intima from advanced fibrous plaque or interpreted the spectra in terms of morphologic and compositional changes that accompany atherosclerosis development.

A few studies measured with time-resolved techniques the fluorescence emission decay of healthy and diseased arterial wall [5–8,12,13]. The time-dependent fluorescence of fibrous atherosclerotic plaque lasted longer than the emission of normal arterial wall [6,7,12]. This observation was thought to reflect the longer lasting emission of collagen relative to that of elastin [8]. The fluorescence decay of healthy arterial wall varied for different wavelengths of excitation and emission to reflect the decay of dominant fluorescent compounds in different wavelength ranges [5]. In most previous studies, the time-resolved fluorescence of artery tissue was only measured for the extreme lesion types and a few wavelengths of emission. The fluorescence decay of lesions in between healthy tissue and advanced fibrous atherosclerosis has been described in a limited way [12,13]. Analysis of the fluorescence decay characteristics for all arterial lesion types and for a broad range of wavelengths would add a second dimension of information to the spectra. The additional information could improve the recognition of different types of atherosclerotic lesions and facilitate the interpretation of tissue spectra in terms of lesion composition and morphology.

Therefore, this study had two main goals. First, we measured the time-resolved fluorescence emission spectra of human aortic samples with graded levels of atherosclerosis and identified characteristic spectral and temporal features for all lesion types ranging from healthy arterial wall to advanced atherosclerotic lesion. Second, we suggested an interpretation for both the spec-

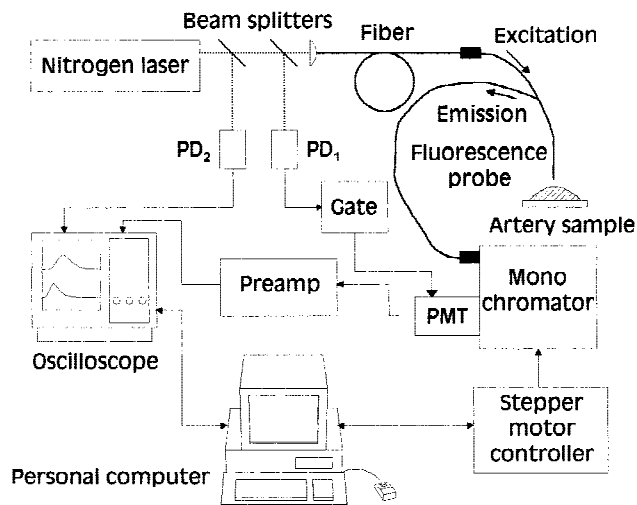


Fig. 1. Spectroscopy setup used to measure the time-resolved fluorescence spectra of aortic tissue samples. PD₁ and PD₂, photodetectors; PMT, multichannel plate photomultiplier tube; Preamp, 1 GHz preamplifier; Gate, gate-and-delay generator.

tral and the temporal features of the fluorescence emission in terms of morphologic and compositional changes that accompany each stage of atherosclerosis development.

MATERIALS AND METHODS

Instrumentation

The laser-induced fluorescence system (Fig. 1) was similar to that used in our previous studies [12–15]. Excitation pulses (3 nsec FWHM) from a free-running nitrogen laser (EG&G, 2100; 10 Hz pulse frequency) were focused on the proximal extremity of a UV-grade silica fiber (core diameter, 600 μm ; NA = 0.22) connected at its distal end to the illumination channel (diameter, 1.4 mm; 200 μm silica fibers; NA = 0.22) of a fluorescence probe (Oriel, 77558). Output from the distal end of the probe illuminated the inner surface of the artery sample (spot size, $\sim 4 \text{ mm}^2$) to produce fluorescence. The broadband emission transient was sampled by a ring of collection fibers (200 μm) around the illumination channel and led to the input slit of a scanning monochromator (Oriel, 77200; F/4.4; UV-Vis grating, 77232; 1,200 grooves/mm; bandpass, 5 nm) for wavelength selection. The emission waveform at the selected wavelength was measured with a gated microchannel plate photomultiplier (Hamamatsu, R2024U; rise time, 0.3 nsec; high voltage, 2.0–2.2 kV) placed against the output slit of the mono-

chromator. The photomultiplier signal was amplified (EG&G Ortec, 9306; rise time, 0.35 nsec; bandwidth, 100 kHz–1 GHz) and sampled with a digitizing oscilloscope (Tektronix, TDS640; bandwidth, 500 MHz; sampling frequency, 2 G samples/sec). A fraction of the laser output was directed toward two silicon photodetectors to gate the photomultiplier (gate duration, 4 μ sec), trigger the oscilloscope, and monitor fluctuations of the laser output energy. A longpass filter (345 nm) at the exit of the monochromator eliminated most of the laser light reflected by the sample. With the monochromator tuned to near the laser line, the amount of reflected light passing through the filter was sufficient to measure the laser pulse waveform.

A personal computer GPIB-interfaced with the wavelength drive controller (Oriol, 77228) and the oscilloscope controlled the tuning of the monochromator and the transfer of data (excitation and emission signals) from the oscilloscope to the computer hard disk. To improve the signal-to-noise ratio of the measurement, the oscilloscope was programmed to average 16 consecutive traces before making the signals available to the computer. After receiving data from the oscilloscope, the computer reset the oscilloscope and shifted the monochromator to the following wavelength of measurement.

Samples

Time-resolved fluorescence spectra were obtained for 94 aortic specimens resected at autopsy from 13 human cadavers (age range, 11–85 years; median age, 48 years) 24–48 hours post mortem. The specimens were abundantly rinsed with buffered saline, cut longitudinally, snap-frozen in isopentane cooled in liquid nitrogen, and stored at -75°C . Before measuring the fluorescence, the samples were allowed to thaw to room temperature. The samples were carefully flattened and pinned to a nonfluorescent plastic board with the intima facing up toward the illumination channel of the fluorescence probe. The samples were examined to select areas with normal or atherosclerotic appearance for the fluorescence study. During the experiment, the samples were maintained moist by dripping buffered saline. After the measurement, small scalpel incisions were made around the illuminated area to identify its location. The samples were fixed in formalin and processed for histologic classification. Hematoxylin and eosin-stained 4- μm -thick transverse paraffin sections cut through the center of the illuminated

regions were classified based on the Stary-American Heart Association classification [16,17] by a pathologist uninformed of the results of the fluorescence study. Six categories were considered: normal aortic wall, type I lesion (initial lesion), type II lesion (fatty streaks), type III lesion (intermediate atheromatous lesion with droplets and small pools of extracellular lipid), type IV lesion (advanced atheroma with extracellular lipid core), and type V lesion (in this study, advanced fibroatheroma with lipid core and collagenous cap; corresponding to type Va in Stary's classification). Samples that did not fall unequivocally in these categories were excluded from further consideration. Calcified lesions (type Vb), which are heterogeneous and yield highly variable emission spectra [4,9], were also excluded. Intimal thickness was measured by quantitative ocular micrometry.

Experimental Procedures

Sample fluorescence was measured at 29 wavelengths (370–510 nm; 5-nm increment) that captured the essential features of aortic wall emission for UV excitation [4]. Ten consecutive measurements of the fluorescence response were recorded at 390, 430, and, 470 nm to compare characteristics of the time-resolved decay across the spectrum of emission. The measurement sequence required 370 seconds to be completed.

The laser energy output at the tip of the fluorescence probe was adjusted to 0.6 $\mu\text{J}/\text{pulse}$. For this energy, the total fluence delivered on the illuminated site was $<0.6 \text{ mJ}/\text{mm}^2$, below the level expected to photobleach the emission of common arterial fluorescent compounds [15]. We verified in a few instances that photobleaching of the sample fluorescence was minimal.

After the fluorescence measurements were completed, the monochromator was adjusted to slightly below the laser line and the laser pulse waveform was recorded. Background noise was measured with the monochromator tuned to 400 nm after removing the sample and lifting the fluorescence probe assembly away from the optical bench. The background noise was subtracted from the laser and fluorescence signals before processing.

Data Analysis

The analysis was composed of two steps. First, we computed the fluorescence impulse response function (IRF) at each wavelength and ordered the IRFs in a two-dimensional array, the

time-resolved fluorescence spectrum, which expressed the variation of the emission intensity as a function of time and wavelength. Second, we applied a global analysis algorithm [18] to find the optimal multiexponential fit of the time-dependent emission decay. The time-resolved fluorescence spectra and the parameters of the fit were compared to identify characteristics of the spectra that differed for the different types of atherosclerotic lesions.

The fluorescence IRF at each wavelength of emission ($h(t, \lambda)$) was retrieved by numeric deconvolution by using the laser excitation waveform as input and the fluorescence emission waveform as output. The deconvolution algorithm has been described and validated in previous work [14,19]. Briefly, the fluorescence IRF was expanded on a basis of discrete-time Laguerre functions [20]. The Laguerre expansion coefficients, which express the contribution of each Laguerre function to the IRF, were computed by a least-squares iterative reconvolution scheme [21]. The algorithm selected values of the coefficients that minimized the squared distance between experimental and modeled fluorescence responses, the latter being represented by the convolution of the IRF with the laser pulse waveform. Seven Laguerre functions were used in the expansion to capture the sub-nanosecond decay dynamics of arterial fluorescence [6,8]. We verified on a representative set of data that, by using more than seven functions, the residual sum of squares between experimental and modeled fluorescence responses did not decrease in comparison with the residual sum of squares obtained with seven Laguerre functions [22]. The time-resolved fluorescence spectrum was constructed by juxtaposing the fluorescence IRFs obtained at the different wavelengths of emission. The raw spectrum was corrected to account for fluctuations of the laser pulse intensity (<5%) and for the nonuniform spectral sensitivity of the measurement system measured with a calibrated irradiance light source (Oriel, 63358). The time-resolved fluorescence spectrum was then normalized to set to 1 the 390-nm intensity at time 0.

A multiexponential approximation of the time-resolved fluorescence spectrum was computed to characterize the decay trends of the time-dependent emission. Under the assumption that the same fluorescent species contribute to the emission for all measured wavelengths, the time decay constants were considered independent of wavelength. The wavelength-dependent preexpo-

nential amplitudes accounted for the variable contribution of each fluorescent species to the overall response. A global analysis algorithm [18,23] was programmed to find optimal values for the decay constants and the preexponential amplitudes by least-squares minimization. Because the fluorescence emission is attenuated for wavelengths between 405 and 445 nm due to increased blood hemoglobin absorption [10], we chose to skip the corresponding portion of the time-resolved spectrum in the estimation of the global decay constants.

Use of three exponentials resulted in trendless residuals [21] and a statistically significant decrease of the residual sum of squares when compared with a biexponential fit [22]. Furthermore, four distinct exponentials could generally not be retrieved from the data or yielded a non-significant reduction of the residual sum of squares. Thus, the global analysis algorithm represented the fluorescence IRF at each wavelength by a three exponential approximation:

$$h(m) = a_S e^{-mT/\tau_S} + a_I e^{-mT/\tau_I} + a_L e^{-mT/\tau_L} \quad (1)$$

where T is the sampling period. The approximation yielded a short (τ_S), an intermediate (τ_I), and a long (τ_L) decay constant for each spectrum. Two wavelength-dependent fractional amplitudes $A_I = a_I / (a_S + a_I + a_L)$ and $A_L = a_L / (a_L + a_S + a_I)$ expressed the relative contributions of the intermediate and the long decay components to the fluorescence IRF. The average lifetime at each wavelength (τ_{avg}) was computed as:

$$\tau_{avg} = \frac{a_S \tau_S + a_I \tau_I + a_L \tau_L}{a_S + a_I + a_L} \quad (2)$$

In addition, the experimental fluorescence emission waveform was integrated numerically as a function of time to compute the cumulative fluorescence intensity at each wavelength. Representation of the cumulative intensity as a function of wavelength yielded the time-integrated emission spectrum, functionally equivalent to the continuous-wave emission spectrum measured with an integrating array detector. The time-integrated spectrum was corrected to account for the wavelength-dependent sensitivity of the detection system and then normalized to set the intensity at 390 nm to 1. The decay constants and preexponential amplitudes were used to compute the decay-associated fluorescence spectra (DAS), which

TABLE 1. Number of Aortic Samples, Subject Age, and Intimal Thickness for the Different Tissue Types*

Sample type	N	Age	Thickness (μm)
Normal	14	32 (11–53)	80 (60–140)
Type I lesion	21	46 (36–63)	120 (80–140)
Type II lesion	19	46 (39–63)	220 (150–280)
Type III lesion	9	56 (39–85)	500 (400–600)
Type IV lesion	5	59 (48–85)	900 (700–1000)
Type V lesion	12	53 (39–85)	1400 (1200–2000)

*Age is reported as mean (minimum–maximum) for all subjects from which the samples of a given type were obtained. Thickness is reported as median value (25th percentile–75th percentile) for each sample type.

expressed the contribution of each decay component to the time-integrated spectrum [23,24].

Decay rates and decay constants were analyzed (one-factor analysis of variance) to evaluate the effect of lesion type on the fluorescence decay. Fractional amplitudes, average lifetime, and DAS intensities at wavelengths 390, 430, and 470 nm were analyzed (one-factor analysis of variance) to evaluate the effect of lesion type in three areas of the emission spectrum. When a significant effect was observed, difference between means was assessed with a post hoc Scheffe test. In all analyses, the level of significance was $P < 0.05$. Data are reported as mean \pm SE.

RESULTS

Histology

Eighty aortic samples were retained after histologic examination and classification. Three of the 14 excluded samples presented extensive calcified lesions and the remaining 11 samples had lesions that could not be unequivocally assigned to one of Sary's classes of atherosclerotic lesions. Partitioning of the 80 retained samples in the different categories of lesions, age range for the corresponding human subjects, and intimal thickness information is provided in Table 1.

Time-Resolved Fluorescence Emission Spectra

Time-resolved spectra of normal aortic wall and atherosclerotic lesions presented characteristic differences in the spectral and the temporal dimensions (Fig. 2). For normal tissue, the emission intensity was maximal at 385 nm and presented a secondary peak at 455 nm that was nearly as high as the main peak of emission. A prominent valley around 415 nm coincided with the Soret absorption maximum of oxyhemoglobin

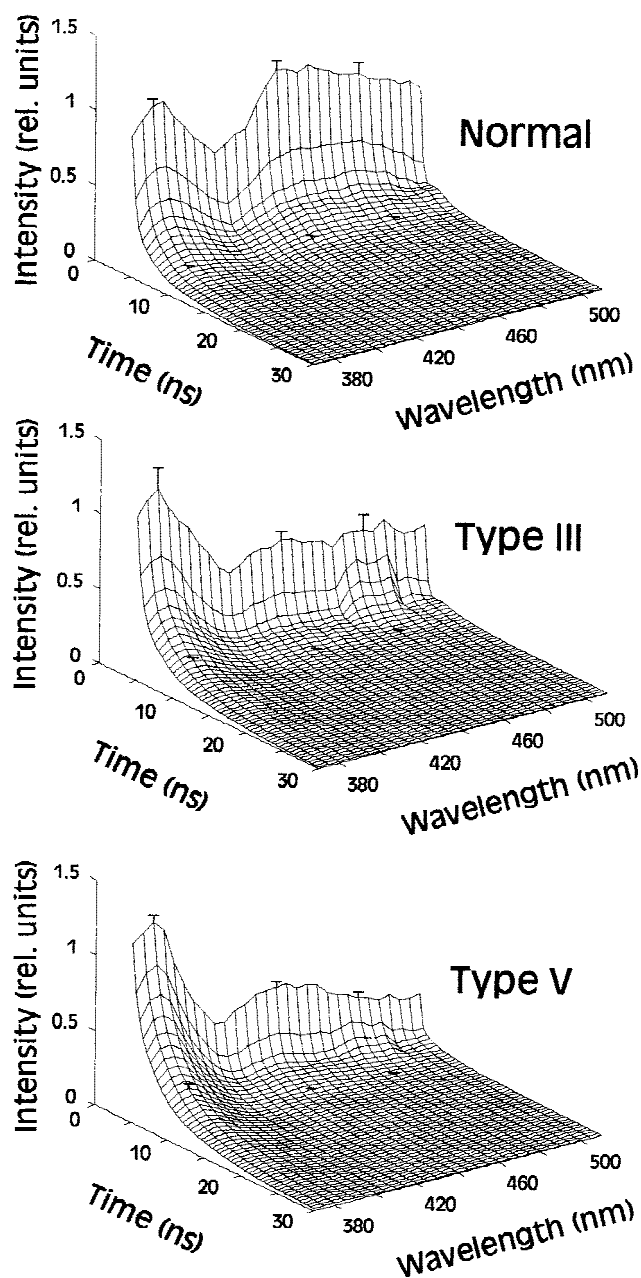


Fig. 2. Normalized time-resolved fluorescence spectra of normal aortic wall (top panel), lipid-rich type III lesion (middle panel), and fibrous type V lesion (bottom panel). Each representation is the average of the normalized time-resolved spectra for all samples of a given type. Standard error of the mean is shown at times 0 and 5 nsec for wavelengths 380, 440, and 480 nm. Intrinsic fluorescence emission intensity varied as a function of time (in nanoseconds) and emission wavelength (in nanometers) in a characteristic manner for each tissue type.

[10]. In the temporal dimension, the emission at 385 nm decayed to 5% of peak intensity in 9.6 ± 0.4 nsec. The rate of fluorescence decay was approximately independent of wavelength. Thus, at

440 nm, the fluorescence decay to 5% of peak intensity occurred in 9.5 ± 0.5 nsec.

For intermediate type III lesions, the main peak of emission was at 380 nm. The secondary peak was less prominent and blue-shifted when compared with the secondary peak in the spectrum of normal tissue. Its intensity was 55% of the main peak intensity and it was reached at 445 nm. The fluorescence decay at the main peak of emission lasted significantly longer than that observed for normal tissue. The intensity decreased to 5% of peak intensity in 12.1 ± 0.7 nsec. In contrast, for wavelengths above 420 nm, the fluorescence duration was similar to that observed for normal tissue (decay to 5% of peak intensity in 10.0 ± 0.5 nsec at 440 nm). For wavelengths between 470 and 490 nm, the rate of fluorescence decay was slower during the first 2 nsec when compared with the rate of decay at neighboring wavelengths.

The main spectral and temporal differences identified between normal tissue and intermediate type III lesions were exacerbated for advanced type V lesions. In these samples, the wavelengths of the primary and secondary peaks were the same as those found in the spectra of type III lesions, but the magnitude of the secondary peak was reduced to 50% of peak intensity. Fluorescence intensity around the peak at 380 nm decayed to 5% of peak intensity in 14.2 ± 0.6 nsec. The rate of fluorescence decay at 440 nm (decay to 5% of peak intensity in 11.2 ± 0.5 nsec) was significantly longer than the decay rates observed for normal tissue and type III lesions at that wavelength. The time-resolved fluorescence spectra of the other types of lesions reflected the progression of changes described from normal aortic tissue to type V lesions.

Decay Constants and Fractional Amplitudes

The short decay constant τ_S (0.4 ± 0.1 nsec) was not different for the different lesion types we examined. In contrast, intermediate and long decay constants significantly varied with lesion type (Fig. 3). Intermediate decay constant τ_I increased by approximately 0.6 nsec for lesion types IV and V when compared with the other lesion types. The largest increase of the long decay constant τ_L (0.9 nsec) was observed between type I and type II lesions.

For all lesion types, fractional amplitude A_I gradually decreased as the emission wavelength increased to 420 nm (Fig. 4a). Parameter A_I reached a plateau between 420 and 465 nm. For

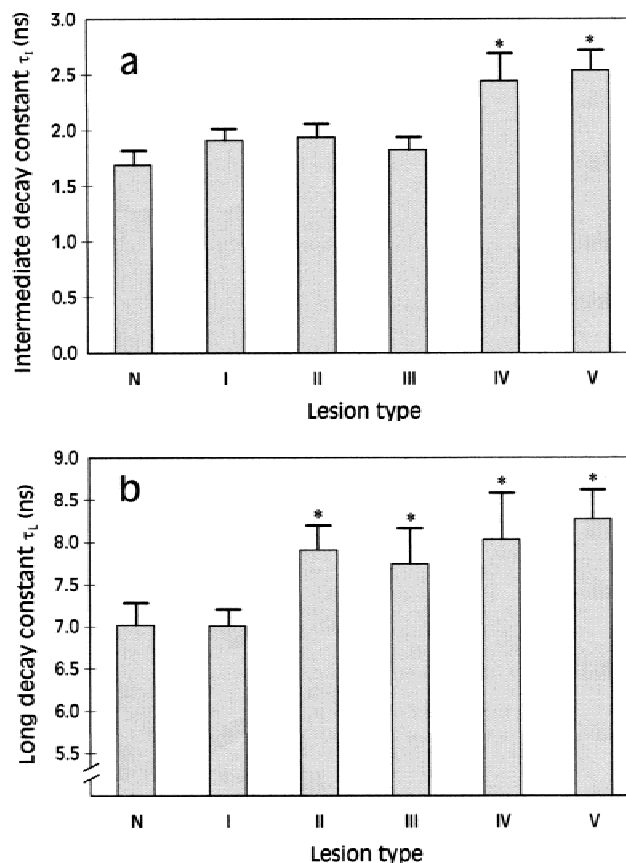


Fig. 3. Decay constants of three-exponential approximation of the time-resolved fluorescence spectra for normal aorta and for atherosclerotic lesions (mean \pm SE). **a:** Intermediate decay constant τ_I . **b:** Long decay constant τ_L . Significant differences associated with the progression of atherosclerosis from normal aorta (N) to type V lesions (V) were observed for both decay constants. Asterisks indicate significant difference compared with normal aorta.

all tissue types, fractional amplitude A_I increased in the 470–490 nm range when compared with the values of A_I in midrange of the spectrum (420–465 nm). The increase was substantially larger for atherosclerotic lesions when compared with normal arterial wall. For wavelengths above 490 nm, amplitude A_I was slightly below the value observed in the midrange of the spectrum.

Fractional amplitude A_L was approximately independent of wavelength for normal arterial wall and type I lesions (Fig. 4b), except for a small dip at 470–490 nm in type I lesions. Type II lesions was associated with a reduced value of A_L over the whole wavelength range when compared with type I lesions. For type III-type V lesions, amplitude A_L at 390 nm was substantially larger than the value of A_L observed for the other tissue types at that same wavelength, A_L being largest

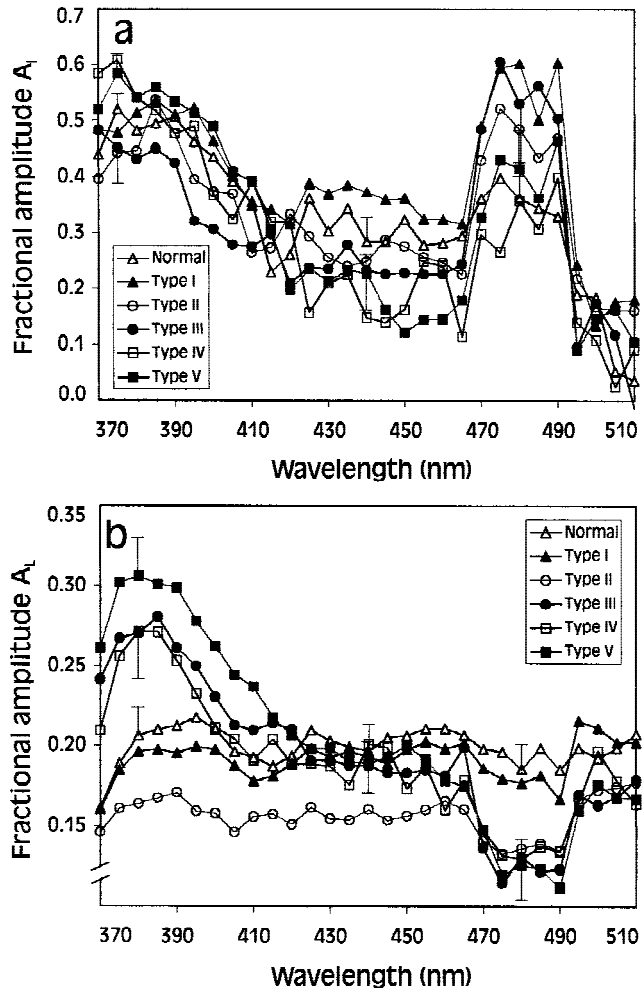


Fig. 4. Wavelength-dependent fractional amplitudes of three-exponential approximation of the time-resolved fluorescence spectra for normal aorta and for atherosclerotic lesions. **a:** Intermediate decay amplitude A_I ; **b:** Long decay amplitude A_L . Each data point is the mean value of the fractional amplitudes for all samples of a given type. To illustrate the variability of the results, the standard error of the mean is plotted for the fractional amplitudes of normal, type III, and type V lesions at 380, 440, and 480 nm.

for type V lesions. For these lesions, fractional amplitude A_L returned to the level observed in normal tissue for wavelengths between 420 and 465 nm. Parameter A_L decreased in the 470–490 nm range in comparison to its midrange values.

Variation of Average Lifetime

The observed variations of the decay constants and fractional amplitudes resulted in the following variations for the average fluorescence lifetime τ_{avg} . For normal arterial wall, type I lesions, and type II lesions, parameter τ_{avg} averaged 2.4 ± 0.1 nsec at 390 nm and decreased to 2.1

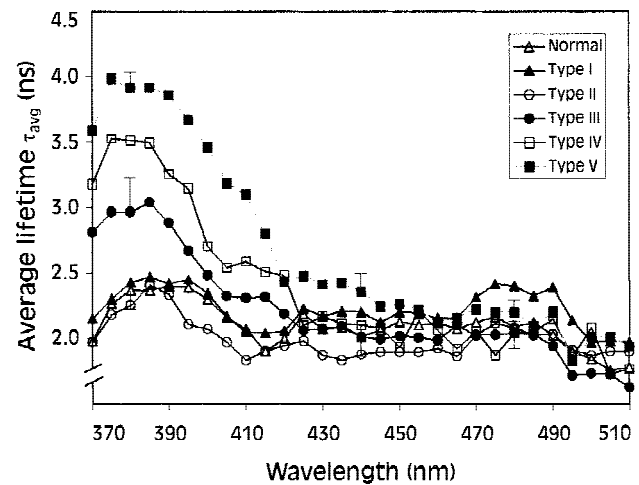


Fig. 5. Average lifetime τ_{avg} as a function of emission wavelength for normal aorta and for atherosclerotic lesions. Each data point represents the mean value of the average lifetimes for all samples of a given type. To illustrate the variability of the results, the standard error of the mean is shown for the lifetime values of normal, type III, and type V lesions at 380, 440, and 480 nm.

± 0.1 nsec at 430 and 470 nm (Fig. 5). The average lifetime measured at 390 nm significantly increased as the severity of the lesion increased to type III and above to reach 3.9 ± 0.1 nsec for type V lesions. For type III and type IV lesions, parameter τ_{avg} measured at 430 nm was not different from the values observed for the less advanced lesion types. For type V lesions, parameter τ_{avg} measured at 430 nm (2.4 ± 0.1 nsec) was larger than the values observed for the other lesion types at that wavelength. At 470 nm, the average lifetime was not different for the different lesion types.

Time-Integrated Emission Spectrum and Decay-Associated Spectra

The time-integrated fluorescence spectrum of normal arterial wall resembled the emission profile observed at time 0 in the time-resolved spectra. The spectrum presented two peaks at 380–385 and 445–450 nm separated by a valley at 415 nm (Fig. 6). The amplitude of the secondary peak was approximately 90% of that of the primary peak. Type I and type II lesions had a slightly more marked primary peak located at 380 nm and a slightly depressed secondary peak when compared with normal aorta. The relative amplitude of the primary peak rose even further for type III–type V lesions to reflect in part the increased duration of the fluorescence decay around

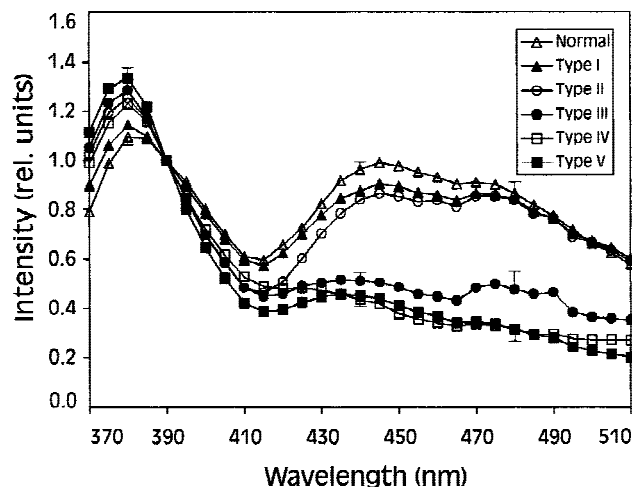


Fig. 6. Normalized time-integrated emission spectra for normal aorta and atherosclerotic lesions. Each data point represents the mean value of normalized emission intensities for all samples of a given type. To illustrate the variability of the results, the standard error of the mean is shown for the emission intensity of normal, type III, and type V lesions at 380, 440, and 480 nm. As the lesion type progresses toward more advanced atherosclerosis, the emission spectra are increasingly more pointed in the blue range and depressed in the red range of the spectrum.

380 nm observed in the more diseased samples. In contrast, the emission intensity in the red range of the spectrum was substantially reduced for intermediate type III lesions and diminished even further for advanced type IV and type V lesions. A small hump between 470 and 490 nm, more noticeable in the spectra of type I-type III lesions, corresponded to the increase of fractional amplitude A_I at these wavelengths.

The DAS of the short decay (not shown) was featureless and $\leq 10\%$ of the whole emission. The DAS of the intermediate decay was markedly depressed at the wavelength of the secondary peak for type III-type V lesions when compared with the less diseased samples (Fig. 7a). The DAS intensity rose between 470 and 490 nm, especially for type I-type III lesions. The DAS of the long decay component had a higher peak of emission around 380 nm (Fig. 7b) and a decreased intensity in the red range of the spectrum for type III-type V lesions when compared with the other lesion types.

DISCUSSION

This study investigated the time-resolved fluorescence spectra of excised samples of human aorta with graded levels of atherosclerosis and

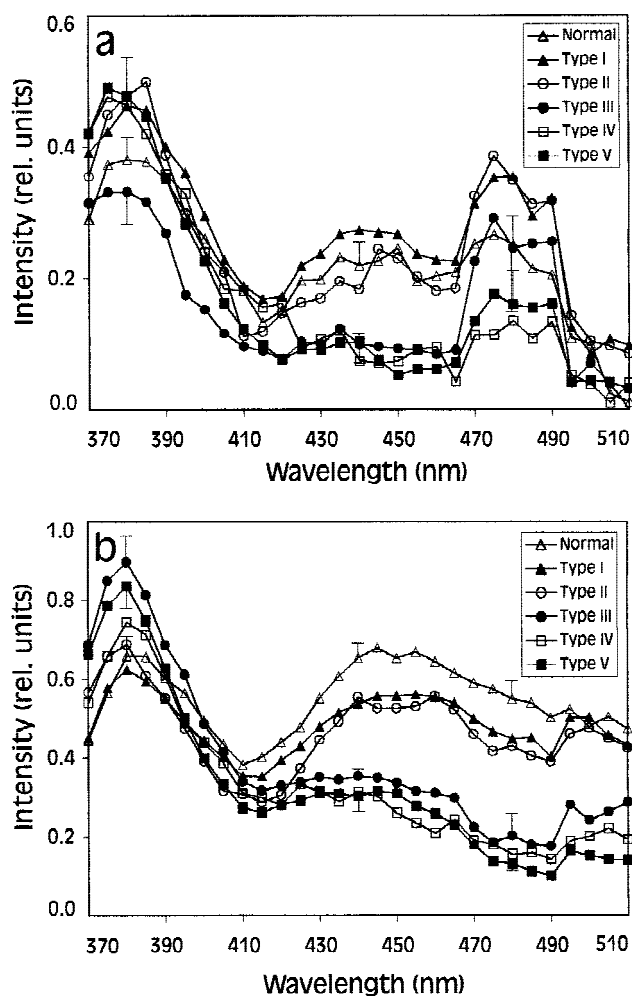


Fig. 7. Decay-associated spectra (DAS) for normal aorta and atherosclerotic lesions are shaped by emission intensity variations as a function of wavelength and time. **a:** intermediate decay DAS. **b:** Long decay DAS. Each data point represents the mean DAS intensity for all samples of a given type. To illustrate the variability of the results, the standard error of the mean is shown for the DAS intensity of normal, type III, and type V lesions at 380, 440, and 480 nm.

identified specific features that characterized the evolution from healthy arterial wall to advanced fibrous atherosclerosis. The principal findings were as follows. First, the time-dependent fluorescence decay lasted longer in the blue range of the spectrum for intermediate and advanced lesions (type III-type V) in comparison with the decay measured in normal aorta and beginning lesions (type I-type II). Second, the fluorescence intensity was markedly decreased in the red range of the spectrum for intermediate and advanced lesions. Third, the rate of fluorescence decay was slower for wavelengths between 470 and 490 nm during the initial phase of the decay in the spectra of

early to intermediate lesions (type I-type III). These modifications resulted in increased exponential decay constants for the atherosclerotic lesions and in alterations of the preexponential terms, average lifetime, and DAS intensities at specific wavelengths.

Methodologic Issues in the Estimation of Time-Dependent Aortic Fluorescence

The time-resolved fluorescence spectra were constructed by using fluorescence decay IRFs estimated by expansion on a Laguerre basis [14,19]. This approach was popularized by Marmarelis [20] who showed that the Laguerre expansion technique was effective at estimating the properties of a dynamic system by using short input-output data records. The Laguerre functions constitute a complete family for the space of square integrable functions. Thus, one is guaranteed that an expansion can be found to represent a fluorescence decay curve of arbitrary shape. In previous work, we established the validity of the Laguerre expansion technique for representing the time-dependent fluorescence of arterial compounds [14,15,25]. In the present study, we showed that the technique could also be applied to compute the intrinsic fluorescence decay of aortic tissue.

Two-dimensional time-resolved fluorescence spectra of aortic tissue measured for different types of atherosclerotic lesions could have been compared by using intensity ratios at selected wavelengths [10,26,27] and times or various shape indices [28]. We chose to approximate the decays by a weighted sum of exponentials from which we derived decay constants, fractional amplitudes, average lifetime, and DAS. Use of a multiexponential approximation allowed us to compare our results with previously obtained characterizations of arterial fluorescence decay [5,6,8]. Note that, in the present study, the exponential approximation of the decay was computed on the IRF expanded on a Laguerre basis rather than as part of the deconvolution of the measured fluorescence transient [5,6]. Early research pointed out that there were advantages in separating the computation of the IRF from the modeling of fluorescence decay in terms of time-dependent processes [29,30].

Multiexponential approximations have been used in different studies to represent the time-dependent decay of arterial fluorescence [5,6,8,12,13]. To the best of our knowledge, the present work is the first in which a global analysis approach [18] was used to estimate the decay con-

stants of the exponential approximation. Global analysis methods take advantage of the relationships that exist between decay curves measured for different values of a parameter (in our case, the emission wavelength). These methods have been proven more accurate in selecting the proper order for the exponential approximation [18,23]. Decay constants and preexponential amplitudes are also more accurately estimated with global analysis [18]. For complex systems like the arterial wall, the decay constants are usually not interpretable in terms of fluorescent species in the system but mainly serve to represent different trends in the decay [31]. Thus, the DAS in the present study may not represent the fluorescence of individual fluorophores in the samples [24]. Use of the DAS was found to be an original and effective way for comparing the fluorescence emission of artery samples by using information from both the spectral and the temporal dimensions.

Spectral Characteristics of Aortic Emission

The time-integrated fluorescence emission spectra of normal aortic wall and atherosclerotic lesions resembled the continuous-wave spectra obtained by different groups with UV excitation ranging from 308 to 337 nm [1–4,9–11,27]. The spectrum of normal aorta was broader than the spectra of lipid-rich and fibrous atherosclerotic lesions [4,9]. Normal intimal spectra usually presented two peaks at 370–410 nm and 430–460 nm [4,9,11,27] separated by a valley around 415 nm. The 415-nm valley was shown to be caused by increased blood absorption around that wavelength [10]. Indeed, normal aortic spectra were found single-peaked in some studies [2], possibly because of differences in sample preparation. The spectra of lipid-rich type III-type IV lesions and fibrous type V lesions were similar [4,9]. The primary peak was located around 380 nm, and the blood absorption valley was less noticeable. The emission in the red range of the spectrum was substantially reduced in comparison with the emission observed in normal tissue, resulting in a single-peaked shape for the spectra. The results of this study are in agreement with these well-documented observations. The present study adds to the state of knowledge in that it describes the fluorescence of aortic samples for all the classes of atherosclerotic lesions between normal arterial wall and advanced fibroatheroma in the Stary classification [16,17]. Use of this fine stratification allowed us to show that the transition from a broad two-peaked spectrum to a narrow single-

peaked spectrum occurred between type II and type III lesions. Gradual changes were identified in the two-peaked spectra of normal, type I, and type II lesions on the one hand and the single-peaked spectra of type III, type IV, and type V lesions on the other.

The time-resolved emission spectra were measured on aortic samples that had been snap-frozen for preservation and slowly thawed just before the experimental measurements. A few studies investigated the effect of freezing-thawing procedures on the fluorescence emission of aortic tissue [10,32]. No substantial differences were found between the emission spectra of fresh samples and those of samples that had been frozen for up to 10 days [32]. Fluorescence emission spectra measured on freshly collected aortic tissue and on frozen samples studied in a cold microtome showed no differences that could be attributed to freezing [33]. These observations suggest that freezing and thawing the aortic samples in the present study did not markedly affect their fluorescence response and contributed slightly if at all to the spectral differences observed between the different types of lesions.

Temporal Characteristics of Aortic Emission

To our knowledge, this study is the first to report the time-resolved fluorescence decay of human aorta over its full spectrum of emission and for all lesion types in the progression of atherosclerosis from normal aortic wall to advanced fibrous lesions [16,17]. Previous investigators examined the time-resolved characteristics of arterial tissue fluorescence only at a few selected wavelengths and for the extreme types of lesions [5–8]. In particular, Andersson-Engels and colleagues [6] used picosecond excitation at 337 nm coupled with single-photon counting detection and an iterative reconvolution scheme [21] to evaluate the fluorescence decay characteristics of aortic and coronary samples at 380, 437, and 480 nm. Normal arterial wall and samples with thin or thick fibrotic plaque, probably type IV and type V lesions, were examined. These authors found, as we did, three exponential components in the fluorescence decays of normal arterial tissue and atherosclerotic lesions. The decay constants of normal samples (380 nm: $\tau_S = 0.2$ nsec, $\tau_I = 1.7$ nsec, $\tau_L = 6.0$ nsec) and thick fibrous lesions ($\tau_S = 0.4$ nsec, $\tau_I = 2.5$ nsec, $\tau_L = 7.5$ nsec) were comparable to the decay constants in our experiments. The main distinction between the time-dependent fluorescence decay of atherosclerotic

lesions and that of normal samples was the 60% increase of fractional amplitude A_L at 380 nm in thick fibrous lesions when compared with normal intima. In the red range of the spectrum, the values of A_L for the different tissue types were nearly equal. These results are in agreement with our observations. In contrast, fractional amplitudes A_I and A_L (0.32 and 0.10 for normal tissue) in the study of Andersson-Engels et al. [6] were approximately 50% smaller than those found in the present work. The average lifetime at 437 nm and 480 nm was markedly decreased for thin fibrotic plaque when compared with normal artery and thick fibrotic plaque in that study. In the present work, the average lifetime was nearly independent of lesion type in the red range of the spectrum. These differences probably originated from experimental and computational differences between the two studies. In particular, aortic and coronary samples were pooled together [6] when these tissues present compositional differences [34] that are likely to affect their fluorescence time-dependent decay.

Because the aortic samples were finely stratified according to lesion type, we were able to show that substantial differences in the time-dependent fluorescence decay were again found between type II and type III lesions. These included differences in the variation pattern of parameters A_L and τ_{avg} with wavelength, coupled with increased values of the average lifetime in the blue range of the spectrum for type III and above lesions. The fact that marked changes in both the spectral and the time-dependent characteristics of fluorescence occur between type II and type III lesions strongly suggests a common interpretation for these changes. Changes of the spectrotemporal fluorescence patterns can be interpreted considering both compositional and morphologic modifications that accompany the development of atherosclerosis from normal arterial wall to advanced fibroatheroma.

Interpretation of Aortic Spectra in Terms of Component Fluorescence

The emission spectrum of normal aortic wall mostly reflects the fluorescence of elastin [2,3,10]. Elastin had a broad spectrum of emission that peaked around 410 nm [2,11]. Its time-dependent decay was represented with two or three exponential terms with decay constants around 1.4 and 6.8 nsec [8,14]. In the artery wall, elastin is primarily located in the deep musculoelastic layer of the intima and in the media [35]. In our normal

samples, intimal thickness was approximately 80 μm . The $1/e$ penetration depth of excitation irradiation around 337 nm is 150–200 μm [10], which suggests that elastin fluorescence from the whole intimal thickness and the media contributed to the emission detected at the luminal surface [9,11]. Other fluorescent compounds that contributed to normal aortic fluorescence probably included collagen and nonelastin matrix proteins, primarily glycosaminoglycans [2,11]. These substances are present in lesser amounts than elastin in normal aorta [2]. However, they are mostly located in superficial layers of the intima near the lumen [35] and, therefore, would be more intensely excited and have their emission less attenuated by absorption and scattering than the emission of elastin. Their contribution shifted the fluorescence peak of normal aortic tissue toward the blue side of the spectrum relative to the elastin peak [11]. The time-integrated spectrum, fluorescence decay constants, and average lifetime measured in our normal samples are in agreement with a dominant role of elastin fluorescence modulated by collagen and glycosaminoglycans emission.

Spectral emission patterns of type I and type II lesions were characterized by an apparent blue shift of the primary fluorescence peak and a small decrease of the secondary peak intensity. Concurrently, intimal thickness increased to 120 nm for type I lesions and 220 nm for type II lesions. Because of the increased intimal thickness, elastin in the musculoelastic layer of the intima and the media would have seen its contribution to intimal fluorescence decrease relatively to the contribution of more superficial collagen and glycosaminoglycans. These compounds have fluorescence spectra that are more narrowly peaked and whose maximal emission is blue-shifted compared with the elastin spectrum [2,11]. Thus, even though intimal content in collagen, nonelastic matrix proteins, and elastin was probably unchanged in type I and type II lesions compared with normal arterial wall [12], the influence of the former compounds on intimal fluorescence increased relative to that of the latter.

The time-dependent parameters changed little for wavelengths below 470 nm in type I and type II lesions compared with normal aorta. Average lifetime did not change, whereas long decay constant τ_L and fractional amplitude A_L increased slightly for type II lesions. Collagen emission lasted longer than that of elastin especially in the blue range of spectrum around 390 nm [8,14]. The

time-dependent fluorescence of glycosaminoglycans has not been described. The emission of these compounds is largely determined by L-tryptophan residues [11] whose fluorescence is short-lived [5,8] such that its decay could be shorter than the decays of elastin and collagen. Overall, the increased contribution of glycosaminoglycans and collagen fluorescence relative to that of elastin would have left the time-dependent decay of type I and type II lesions relatively unchanged. For wavelengths between 470 and 490 nm, marked increases of the fractional amplitude A_I and of the intermediate decay DAS intensity were observed. Marcu et al. [25] reported that fluorescence emission of free cholesterol and cholesterol esters increased in that wavelength range and was associated with the appearance of a delay in the time-dependent emission. Type I and type II lesions are characterized by the intracellular accumulation of lipid droplets in the intima, primarily cholesterol esters, free cholesterol, and phospholipids [16]. Our results seem to indicate that fluorescence from these lipids was noticeable in the time-resolved fluorescence characteristics of intimal emission and changed parameter A_I and the intermediate DAS intensity for wavelengths between 470 and 490 nm. Lipid fluorescence would have also contributed to narrowing and blue shift of the spectral peak to 380 nm [25]. Note that in the 470- to 490-nm band, the change of parameter A_I and of the intermediate decay DAS from normal aortic wall to type I and type II lesions was much more marked than the intensity variation in the time-integrated spectra. This observation suggests that measurement of the time-resolved spectra would improve the ability to detect beginning atherosclerotic lesions.

As indicated in the preceding section, the transition from type II to type III lesions was accompanied by dramatic changes in the shape of the time-integrated spectrum and in the patterns of variation of parameters A_L and τ_{avg} with wavelength. These variations were reflected in marked changes of the intermediate and long decay DAS. The observed differences do not appear to originate in changes of the tissue fluorophore content between the two lesion types. Histologically, the main difference between type II to type III lesions is the accumulation of lipids in extracellular droplets and small pools [16]. Compositional changes are thought to be small [16]. Rather the spectrotemporal differences would reflect a marked change of the intimal thickness that increased

from 220 μm for type II lesions to 500 μm for type III lesions in our samples. Whereas the tissue volume probed by the fluorescence measurement included both subluminal intima and deep intima in type II lesions, this volume became mostly located in the subluminal intima in type III lesions. Thus, whereas elastin from the deep intima and possibly the media strongly contributed to the spectra of type II lesions, the emission of type III lesions was mostly determined by fluorescent compounds in the subluminal intima, collagen, glycosaminoglycans, and lipids. The three compounds would have yielded the single-peaked spectrum and the increased values of parameters A_L and τ_{avg} . Fluorescence from the lipids would have resulted in increases of fractional amplitude A_I and the intermediate decay DAS between 470 and 490 nm. Previous studies had highlighted the role played by elastin from the media in shaping the fluorescence spectrum of normal arterial wall and early atherosclerotic lesions. [2,9,11]. Our results pinpoint the stage in the progression of atherosclerosis where elastin ceased to be a significant contributor to the aortic spectra, i.e., between type II and type III lesions.

Fluorescence emission of type IV lesions was characterized by a further decline of the emission intensity around the secondary peak, which practically ceased to be a defining feature of the time-integrated spectra. In the time dimension, intermediate decay constant τ_I and average lifetime τ_{avg} were increased compared with their values in type III lesions. The contribution of lipid fluorescence around 470–490 nm was less noticeable than was observed for type III lesions, especially in the DAS. Type IV lesions are characterized by increased accumulation of lipids and formation of a lipid core [17] with no increase in fibrous collagen. The lipid core is usually located under a well-defined layer of cells and matrix material containing collagen and proteoglycans. It is likely that the fluorescence measurement reflected an increased contribution of the latter two compounds. Lipids in the core were so deeply located in the intima that their contribution to the fluorescence measurement actually diminished in comparison with the contribution detected in type III lesions. Note that we had only five aortic samples classified as type IV lesions such that further study would be needed to confirm this observation. The spectrotemporal emission of type V lesions was characterized by further increases of parameter A_L and of the average lifetime, which reflected the dominant contribution of fibrous collagen at the

intimal surface [2,8,11]. To our knowledge, the present interpretation is the first that examines the combined changes of the spectral and the temporal fluorescence emission patterns of aortic tissue for the full progression of atherosclerotic lesions established by histologic observations [16,17]. This interpretation shows that compositional changes that accompany the development of atherosclerotic lesions condition only partly the fluorescence variations. Key roles are also played by intimal thickness changes and by the propagation of excitation and fluorescence light within the intimal thickness [36].

Note that even though the elastin content of human aorta decreases with age relative to the collagen content [35], this factor probably had a minimal effect on the fluorescence emission differences that marked the progression from type I to type V lesions. For these lesion types, the aortic samples in the present study were obtained from adult subjects of comparable age at the time of death (Table 1). Some of the normal samples originated from a juvenile, which could have contributed in part to the small differences noted between the fluorescence spectra of normal samples and those of type I lesions.

Implications for optical analysis of the arterial wall

The first implication of our results is that analysis of the time-resolved fluorescence spectra can be used to enhance the optical differentiation between graded levels of atherosclerosis. Previous reports had established that continuous-wave fluorescence spectra could be used to differentiate between normal aortic wall and advanced atherosclerotic lesions [1,2,27]. A few studies had shown that lipid-rich lesions could be recognized from the other lesion types [4,11] and that the time-resolved fluorescence emission of fibrous lesions was different from that of normal arterial wall [6,8]. The present study examined the time-dependent emission of early and lipid-rich aortic lesions (type I-type IV). Specific features were identified in the time-resolved spectra to distinguish these lesions from normal aorta and from advanced fibrous lesions. Combined use of the spectral and the temporal characteristics of the emission could serve to precisely and nondestructively assign an aortic fluorescence measurement to a class of atherosclerotic lesion known to have well-defined histologic and morphologic features [16,17].

The second implication of this study is that

measurement of the time-resolved fluorescence spectra of aortic samples yields an abundance of parameters such that proper data reduction can help in extracting the most distinctive features of the spectra. We suggest that the average lifetime as a function of wavelength curve and the DAS of the intermediate and long decays could suffice to identify aortic lesions. The lifetime characterizes the overall rate of emission decay at different wavelengths and the DAS combine spectral and temporal attributes of time-resolved emission. Type III and above lesions would be recognized from normal aortic wall and less advanced lesions by a decreased emission between 430 and 470 nm in the DAS curves and by increased lifetime values around 390 nm. Type I and type II lesions would yield in the long decay DAS a reduced emission in the 430–470 nm range when compared with normal aortic wall. Increased emission between 470 and 490 nm would be observed in the intermediate decay DAS. The progression from type III to type V lesions would translate in an increased lifetime around 390 nm that extends further toward the red range of the spectrum. Reduced emission in the 470- to 490-nm range would be noted in the intermediate decay DAS. The lifetime and DAS data could be used in the development of algorithms for automatic classification of atherosclerotic lesions [3,10,27].

The third implication is that the organization and thickness of the different layers in the arterial wall cross-section is as important as their content in fluorescent materials in determining the time-resolved fluorescence spectrum of the tissue. The sequence of spectrottemporal fluorescence changes identified in our aortic samples might need to be revisited for other arterial segments such as the coronary vessels. The elastin to collagen ratio is different in these vessels when compared with normal aorta, which leads to known spectral differences [34], but also the coronary wall is much thinner than the aortic wall. It is conceivable, for instance, that elastin from the deep intima could contribute to the emission of type III lesions in coronary arteries even though elastin was too deeply buried to affect the fluorescence spectra of such lesions in the aorta. Furthermore, artery tissue is stretched longer and thinner in vivo such that the role of tissue thickness would need to be reassessed for proper interpretation of time-resolved fluorescence spectra measured in situ. Development of an optical biopsy system for in situ assessment of atherosclerotic lesions will need to take into account both

the artery bed and the experimental conditions in which the device is used. Yet, clinical studies [4,28] have demonstrated the feasibility of measuring in situ the continuous wave fluorescence emission of coronary artery vessels during percutaneous catheterization. The fluorescence spectra of atherosclerotic coronary artery measured in situ resembled the emission spectra obtained in vitro on excised coronary specimens and reflected the lesion type evaluated independently with intracoronary ultrasound [28]. These reports demonstrate that intracoronary fluorescence measurements are possible and yield clinically useful information. The present work suggests that in situ measurement of the time-dependent characteristics of the fluorescence would allow for a more precise staging of atherosclerotic lesions and thus enhance the diagnostic capability of fluorescence spectroscopy.

CONCLUSION

This study established that the time-resolved fluorescence emission spectra of aortic samples vary with the progression of atherosclerosis. Characteristic changes in parameters derived from the time-resolved spectra were related to the type of lesion assigned to the sample based on histologic examination. Spectral and temporal features of the emission were interpreted for normal aortic wall and lesions ranging from early type I to advanced type V in terms of intimal content in fluorescent compounds and intimal thickness. Trends in the average lifetime and decay-associated spectra at selected wavelengths were identified, which could serve as diagnostic markers for in situ optical analysis of the aortic wall.

REFERENCES

1. Kittrell C, Willett RL, de los Santos-Pacheco S, Ratiff NB, Kramer JR, Malk EG, Feld MS. Diagnostic of fibrous arterial atherosclerosis using fluorescence. *Appl Opt* 1985; 24:2280–2281.
2. Laifer LI, O'Brien KM, Stetz ML, Gindi GR, Garrand TJ, Deckelbaum LI. Biochemical basis for the difference between normal and atherosclerotic arterial fluorescence. *Circulation* 1989;80:1893–1901.
3. Yan WD, Perk M, Chapgar A, Wen Y, Stratoff S, Schneider WJ, Jugdutt BI, Tulip J, Lucas A. Laser-induced fluorescence: III. Quantitative analysis of atherosclerotic plaque content. *Lasers Surg Med* 1995;16: 164–178.
4. Morguet AJ, Gabriel RE, Buchwald AB, Werner GS, Nyga R, Kreuzer H. Single-laser approach for fluorescence guidance of excimer laser angioplasty at 308 nm: evaluation in vitro and during coronary angioplasty. *Lasers Surg Med* 1997;20:382–393.

5. Baraga JJ, Taroni P, Park YD, An K, Maestri A, Tong LL, Rava RP, Kittrell C, Dasari RR, Feld MS. Ultraviolet laser induced fluorescence of human aorta. *Spectrochim Acta A* 1989;45:95–99.
6. Andersson-Engels S, Johansson J, Svanberg S. The use of time-resolved fluorescence for diagnosis of atherosclerotic plaque and malignant tumours. *Spectrochim Acta A* 1990;46:1203–1210.
7. Andersson-Engels S, Johansson J, Svanberg K, Svanberg S. Fluorescence imaging and point measurements of tissue: applications to the demarcation of malignant tumors and atherosclerotic lesions from normal tissue. *Photochem Photobiol* 1991;53:807–814.
8. Andersson-Engels S, Baert L, Berg R, D'Hallewin MA, Johansson J, Stenram U, Svanberg K, Svanberg S. Fluorescence characteristics of atherosclerotic plaque and malignant tumors. *SPIE* 1991;1426:31–43.
9. Laufer G, Wollenek G, Hohla K, Horvat R, Henke KH, Buchelt M, Wutzl G, Wolner E. Excimer laser-induced simultaneous ablation and spectral identification of normal and atherosclerotic arterial tissue layers. *Circulation* 1988;78:1031–1039.
10. Baraga JJ, Rava RP, Taroni P, Kittrell C, Fitzmaurice M, Feld MS. Laser induced fluorescence spectroscopy of normal and atherosclerotic human aorta using 306–310 nm excitation. *Lasers Surg Med* 1990;10:245–261.
11. Oraevsky AA, Jacques SL, Pettit GH, Sauerbrey RA, Titte FK, Nguy JH, Henry PD. XeCl laser-induced fluorescence of atherosclerotic arteries: spectral similarities between lipid-rich lesions and peroxidized lipoproteins. *Circ Res* 1993;72:84–90.
12. Maarek JM, Marcu L, Grundfest WS. Characterization of atherosclerotic lesions with laser-induced time resolved fluorescence spectroscopy. *SPIE* 1998;3250:181–189.
13. Marcu L, Maarek JM, Fishbein M, Grundfest WS. Atherosclerotic lesions classification by time-resolved laser induced fluorescence spectroscopy: clinical identification of lipid-rich lesions. *J Am Coll Cardiol* 1999;33:66A.
14. Maarek JM, Snyder WJ, Grundfest WS. Time-resolved laser-induced fluorescence of arterial wall constituents: deconvolution algorithm and spectro-temporal characteristics. *SPIE* 1997;2980:278–285.
15. Marcu L, Grundfest WS, Maarek JM. Photobleaching of arterial fluorescent compounds: characterization of elastin, collagen, and cholesterol time-resolved spectra during prolonged ultraviolet irradiation. *Photochem Photobiol* 1999;69:713–721.
16. Sary HC, Chandler AB, Glagov S, Guyton JR, Insull W Jr, Rosenfeld ME, Schaffer SA, Schwartz CJ, Wagner WD, Wissler RW. A definition of initial, fatty streak, and intermediate lesions of atherosclerosis. *Arterioscler Thromb* 1994;14:840–856.
17. Sary HC, Chandler AB, Dinsmore RE, Fuster V, Glagov S, Insull W Jr, Rosenfeld ME, Schwartz CJ, Wagner WD, Wissler RW. A definition of advanced types of atherosclerotic lesions and a histological classification of atherosclerosis. *Arterioscler Thromb Vasc Biol* 1995;15:1512–1531.
18. Knutson JR, Beechem JM, Brand L. Simultaneous analysis of multiple fluorescence decay curves: a global approach. *Chem Phys Lett* 1983;102:501–507.
19. Snyder WJ, Maarek JM, Papaioannou T, Marmarelis VZ, Grundfest WS. Biologic fluorescence decay characteristics: determination by Laguerre expansion technique. *SPIE* 1996;2679:150–161.
20. Marmarelis VZ. Identification of nonlinear biological systems using Laguerre expansions of kernels. *Ann Biomed Eng* 1993;21:573–589.
21. Grinvald A, Steinberg IZ. On the analysis of fluorescence decay kinetics by the method of least squares. *Anal Biochem* 1974;59:583–598.
22. Landaw EM, DiStefano JJ 3rd. Multiexponential, multi-compartmental, and noncompartmental modeling. II. Data analysis and statistical consideration. *Am J Physiol* 1984;246:R665–R677.
23. Vermunicht G, Boens N, De Schryver FC. Global analysis of the time-resolved fluorescence of α -chymotrypsinogen A and α -chymotrypsin powders as a function of hydration. *Photochem Photobiol* 1991;53:57–63.
24. Knutson JR, Walbridge DG, Brand L. Decay-associated fluorescence spectra and the heterogeneous emission of alcohol dehydrogenase. *Biochemistry* 1982;21:4671–4679.
25. Marcu L, Maarek JM, Grundfest WS. Time-resolved laser induced fluorescence of lipids involved in development of atherosclerotic lesion lipid-rich core. *SPIE* 1998;3250:158–167.
26. Morguet AJ, Körber B, Abel B, Hippler H, Wiegand V, Kreuzer H. Autofluorescence spectroscopy using a XeCl excimer laser system for simultaneous plaque ablation and fluorescence excitation. *Lasers Surg Med* 1994;14:238–248.
27. Deckelbaum LI, Stetz ML, O'Brien KM, Cutruzzola FW, Gmitro AF, Laifer LI, Gindi GR. Fluorescence spectroscopy guidance of laser ablation of atherosclerotic plaque. *Lasers Surg Med* 1989;9:205–214.
28. Bartorelli AL, Leon MB, Almagor Y, Prevosti LG, Swain JA, McIntosh CL, Neville RF, House MD, Bonner RF. In vivo human atherosclerotic plaque recognition by laser-excited fluorescence spectroscopy. *J Am Coll Cardiol* 1991;17:160B–168B.
29. Ware WR, Doemeny LJ, Nemzek TL. Deconvolution of fluorescence and phosphorescence decay curves: a least-squares method. *J Phys Chem* 1973;77:2038–2048.
30. James DR, Ware WR. Recovery of underlying distribution of lifetimes from fluorescence decay data. *Chem Phys Lett* 1986;126:7–11.
31. Lakowicz JR. Principles of fluorescence spectroscopy. New York: Plenum Press; 1983. p 51–91.
32. Leon MB, Lu DY, Prevosti LG, Macy WW Jr, Smith PD, Granovsky M, Bonner RF, Balaban RS. Human arterial surface fluorescence: atherosclerotic plaque identification and effects of laser atheroma ablation. *J Am Coll Cardiol* 1988;12:94–102.
33. Cutruzzola FW, Stetz ML, O'Brien KM, Gindi GR, Laifer LI, Garrand TJ, Deckelbaum LI. Changes in laser-induced arterial fluorescence during ablation of atherosclerotic plaque. *Lasers Surg Med* 1989;9:109–116.
34. Garrand TJ, Stetz ML, O'Brien KM, Gindi GR, Laifer LI, Deckelbaum LI. Characterization of the site dependency of normal canine arterial fluorescence. *Lasers Surg Med* 1990;10:375–383.
35. Sary HC, Blankenhorn DH, Chandler AB, Glagov S, Insull W Jr, Richardson M, Rosenfeld ME, Schaffer SA, Schwartz CJ, Wagner WD, Wissler RW. A definition of the intima of human arteries and of its atherosclerosis-prone regions. *Circulation* 1992;85:391–405.
36. Richards-Kortum R, Rava RP, Cothren R, Metha A, Fitzmaurice M, Ratliff NB, Kramer JR, Feld MS. A model for extracting of diagnostic information from laser induced fluorescence spectra of human artery wall. *Spectrochim Acta A* 1989;45:87–93.